Int. J. Multiphase Flow Vol. 14, No. 4, pp. 389–400, 1988
Printed in Great Britain

0301-9322/88 $3.00 + 0.00
Pergamon Press/Elsevier

GAS–LIQUID FLOW AT MICROGRAVITY CONDITIONS: FLOW PATTERNS AND THEIR TRANSITIONS

A. E. DUKLER,[1] J. A. FABRE,[1]† J. B. MCQUILLEN[2] and R. VERNON[2]
[1]University of Houston, Houston, TX 77004, U.S.A.
[2]Lewis Research Center, Cleveland, OH 44235, U.S.A.

(*Received* 24 *January* 1988; *in revised form* 19 *April* 1988)

Abstract—The prediction of flow patterns during gas–liquid flow in conduits is central to the modern approach for modelling two-phase flow and heat transfer. The mechanisms of transition are reasonably well understood for flow pipes on earth where it has been shown that body forces largely control the behavior observed. This work explores the patterns which exist under conditions of microgravity when these body forces are suppressed. Data are presented which were obtained for air–water flow in tubes during drop tower experiments and Learjet trajectories. Preliminary models to explain the observed flow pattern map are evolved.

Key Words: two-phase flow, flow pattern, microgravity

INTRODUCTION

The existence of two-phase gas–liquid flow is anticipated for a wide variety of applications in space, including:

- Cryogenic transfer and storage, particularly transfer line cooldown for experiments located in fixed orbit which must be periodically resupplied.
- Heat transfer associated with space nuclear power facilities during steady-state operation and during emergencies due to unanticipated loss-of-coolant accidents.
- Design and operation of a thermal bus for the space station. The bus is intended to supply a utility heat sink for a wide variety of, as yet unspecified, processes.
- Design of life-support systems.
- Gas–liquid separations in space.
- Condensation and flow boiling processes.

In order to design or predict performance of equipment for these applications, as well as many others, it will be necessary to have models which give a detailed description of the mechanics of such flows. Of most general interest is the manner in which the phases distribute (the flow patterns), and the pressure drop and its fluctuation. But there are situations where much more detailed information may be necessary, including the size and velocity of the liquid slugs if they exist as well as the forces generated on the confining equipment and their characteristic frequency. When bubbles or drops are present it is frequently required to have information about their size and velocity, including an analysis of the heat and mass transfer accompanying the flow. If annular flow takes place, of importance are models for the interfacial shear, the interfacial wave structure, the velocity distribution in the two phases, the radial distribution of bubbles or drops and an understanding of the process of droplet creation from the continuous liquid phase.

During the past 10 years there has been an extraordinary amount of attention paid to modelling gas–liquid flow under normal gravity conditions. Physically based models now exist or will exist shortly for many of the situations described above. However, on earth the force due to gravity plays a dominant role in controlling the behavior of two-phase systems. For example, over a fairly wide range of flow rate space the flow pattern of gas–liquid flow in a horizontal tube can change drastically when the pipe is inclined upward as little as 1° from the horizontal (Taitel & Dukler 1976). Even at this small inclination, the component of the force of gravity acting in the axial direction exceeds the force due to wall shear stress. Clearly, this condition will not exist at microgravity.

†Present address: Institut de Mécanique des Fluides de Toulouse, Toulouse, France.

Calculations show that in larger conduits (say, above 2.5 cm/dia) at 1 G the forces along the free surfaces are usually small compared to the inertial and gravity forces that act. This has been confirmed by numerous studies that show a weak influence of interfacial tension on pressure drop, holdup and flow patterns. For microgravity this condition can also be expected to be different.

Thus, it becomes necessary to reexamine existing models which describe the character of gas–liquid flow on earth and to modify or construct new ones to provide valid descriptions of what happens at microgravity. Essential to a process as complex as this one is the acquisition of reliable experimental data to provide insight into mechanisms on which physical models can be based and which can be used to test the results.

This paper presents the results of the first phase of this strategy of engineering research carried out under the sponsorship of the NASA Lewis Research Center. Discussed here are the results of a study of flow patterns. Experimental data were obtained in drop tower tests and in the LERC Learjet. Work is continuing both on flow pattern transition modelling and on other aspects of the problem.

SOME RELATED STUDIES

Research on the effect of reduced gravity on pool nucleate boiling seems to have been initiated by Siegal & Usiskin (1959). About 25 papers and reports appeared between 1959 and the contribution of Weinzierni & Straub in 1982. Considerable experimental data now exist. In contrast, the published research on either experiments or modelling for the *flow* of two phases is sparse. Albers & Macosko (1965, 1966) measured the pressure drop of condensing mercury at zero gravity, while Namkoong *et al.* (1987) made a photographic study of the zero-gravity mercury condensation process. Williams *et al.* (1973) reported the condensation of R-12 in a tube, 2.62 mm dia × 1.83 m long, at 1 G and showed a single C-135 aircraft trajectory experiment. Qualitative comparisons were made for the two conditions.

The most extensive work on zero-gravity gas–liquid flow was presented by Hepner *et al.* (1975, 1978). C-135 trajectories were used to collect data on flow patterns for air–water flow in a 2.54 cm dia tube having an L/D of 20. Although the test section length was short and duplicate tests gave significantly different results, the work is a landmark study. Unfortunately, the original films apparently are no longer available. Over the past 10 years improved methods have been developed to interpret high-speed films taken of two-phase flow. Thus, if available, it is likely that these films would be interpreted differently today.

There have recently been a variety of conceptual studies on flow pattern transitions in space, usually connected with proposed hardware design for space experiments. However, these offer little in the way of new insights. Lovell (1985) attempted to construct an experimental analog of zero-gravity two-phase flow by using two fluids of near identical density (water and polypropylene glycol). Experiments were carried out in a glass tube, 2.54 cm dia × 6.3 m long. Serious questions must be raised as to the validity of the simulation.

EXPERIMENTAL EQUIPMENT

Experiments were carried out both on the Lewis 100 ft drop tower and on the Lewis Learjet using water and air. The data from both experimental loops consisted of the flow rates, temperatures, movie films taken at about 400 frame/s along with time-dependent pressure drop data. However, a much greater level of detail during each run was obtained in the Learjet tests because it was possible to construct a larger experimental rig equipped with a more complete data acquisition system. The drop tower provided about 2.2 s of near-zero gravity, while with the Learjet it was possible to collect data over 12–22 s depending on the quality of the particular trajectory. Accelerometer measurements, taken with run, made it possible to limit data acquisition on the Learjet to periods when the acceleration did not exceed +0.02 G in any of the three principal coordinates of the plane.

A schematic diagram of the drop tower loop is shown in figure 1. The test section consisted of a transparent Plexiglas tube, 9.52 mm dia × 0.457 m long, which was backlit. At the mixer, air was injected into the liquid through four peripheral holes. Flow rates were set while the rig was

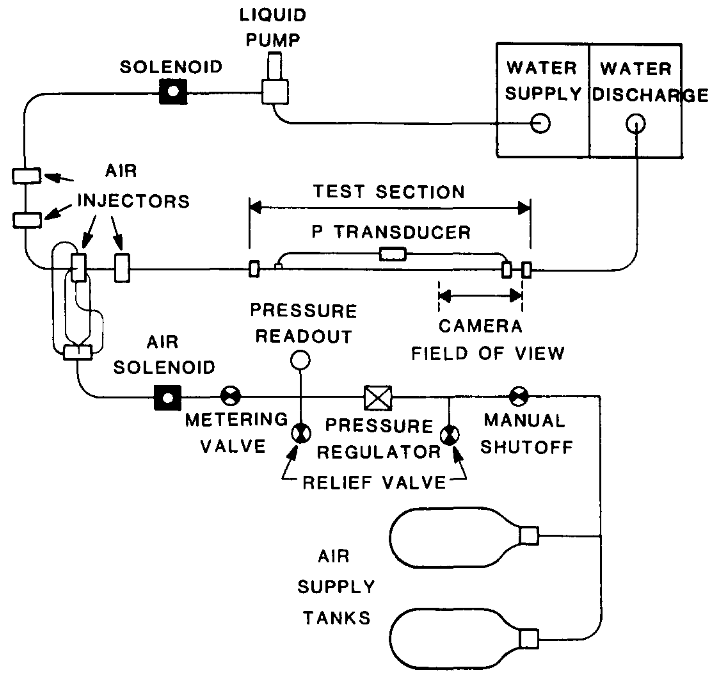

Figure 1. Drop tower flow loop.

suspended on its platform at the top of the tower. A calibrated valve was used for regulating air rate while the speed of a voltage-controlled centrifugal pump regulated the liquid flow rate. A film record was taken at this 1 G condition. Then without changes in the settings the drop was executed with the camera activated. The rig was not equipped with flowmeters and it was assumed that the pump speed and flow through the air control valve would not change during the drop. Subsequent analysis indicated that due to drawdown of the batteries during the drop, the pump speed did change for certain runs. The pressure drop measuring system was not equipped with water flushing for the lead lines and the data thus collected was not considered reliable enough to use in the analysis.

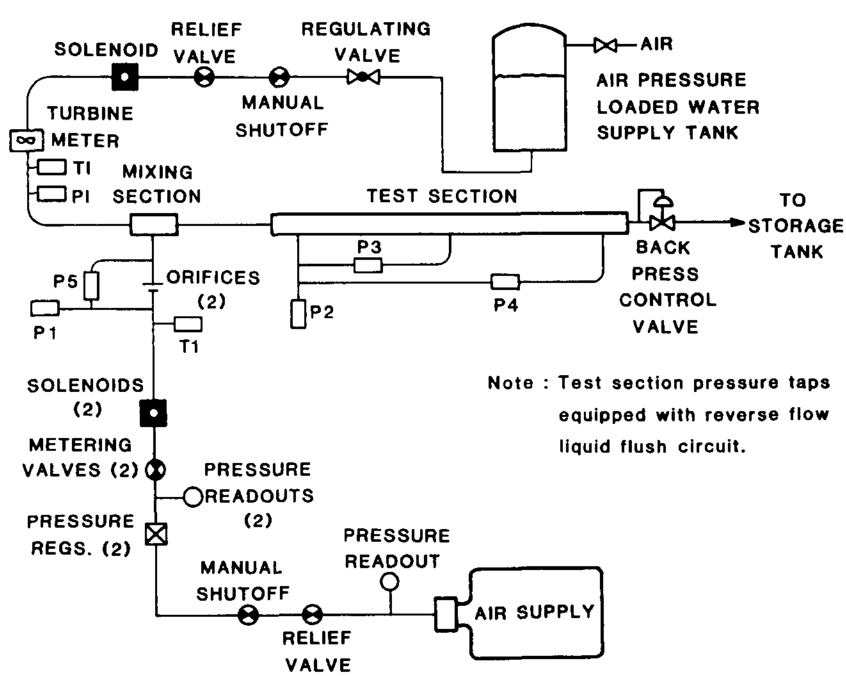

Figure 2. Learjet flow loop.

The test loop for the Learjet, whose schematic diagram is shown in figure 2, was designed to overcome many of the limitations revealed from the drop tower experience. Air flow was metered through two critical flow orifices (one for high and one for low flow rates) with liquid measured using a turbine meter. Readings of the flow and temperature transducers were taken continually at 1.55 s intervals during the run. The test section pressure taps were equipped with reverse flush circuits which were activated just before the trajectory reached zero gravity. Varian pressure transducers were used for measuring these pressure drops. Test section pressure drop data was collected at intervals of 0.002 s. The total straight length of the test section was 1.06 m, with dia 12.7 mm. The transparent test section was backed by a meter stick marked in millimeters and the rig was equipped with an LED display which indicated the elapsed time in 0.01 s intervals. Color films were taken at 400 frame/s. Thus it was possible to obtain, in addition to flow pattern indications, measurements of the velocities of slugs, bubble and interfacial waves as well as sizes of bubbles and slugs. In these measurements corrections for parallax errors were made. For each run at normal gravity a corresponding run was executed at zero gravity at the same gas and liquid rate after the rig had been removed from the Learjet.

A study of the films showed that the flow patterns and the other characteristics of the flow were unchanging after the first 1–1.2 s into microgravity conditions. The calculated passage time for a continuity wave to traverse the test section was never greater than 1.2 s and is thus consistent with this determination.

QUALITATIVE OBSERVATIONS

Table 1 summarizes the flow conditions for the tests which were carried out in the drop tower, and Table 2 those executed in the Learjet. Included is the flow pattern as deduced from a study of the films. Bubbly flow is designated when the gas bubbles are of a size less than or equal to the tube diameter. The term slug flow is used when there exist gas bubbles greater in length than the tube diameter and where there are regions along the tube where the liquid completely covers the flow area of the tube, even though this liquid may carry dispersed gas bubbles. Annular flow is the condition where the liquid never bridges the tube.

The information obtained from a study of the movie films is arrived at, in part, by observing a sequence of successive frames. However, in order to convey at least part of the impression, a series of black-and-white stills have been prepared and are presented in this section. Since these black-and-white photographs are very inferior copies of the original color pictures and only represent a single observation over a 1/400 s interval, hand traces of a different frame for each run have also been prepared to illustrate some details and the diversity of appearance.

Figure 3A shows photographs of single frames taken from the films for four gas rates at a low liquid rate of about 0.08 m/s. Hand traces of different frames in the same runs are shown in figure

Table 1. Drop tower runs

RUN #	U_{GS} (m/s)	U_{LS} (m/s)	FLOW PATTERNS	Re_G	Re_L
1	0.252	0.657	BUBBLE :1D B	231	8344
2	0.252	0.444	BUBBLE :1D B	231	5639
3	0.252	0.278	SLUG : 2D-4D TB	231	3531
4	0.421	0.562	BUBBLE :1D B	386	7137
5	0.421	0.369	SLUG : short slugs	386	4686
6	0.421	0.171	SLUG : short slugs	386	2172
7	0.230	0.950	BUBBLE	211	12065
8	0.230	0.749	BUBBLE	211	9512
9	0.230	0.532	BUBBLE	211	6756
10	0.230	0.250	BUBBLE	211	3175
12	0.460	0.697	BUBBLE	422	8852
13	0.460	0.442	BUBBLE	422	5613
14	0.460	0.175	SLUG :1D TB	422	2223
16	0.690	0.598	SLUG : 2D TB	633	7595
17	0.690	0.366	BUBBLE :1D B	633	4648
18	0.690	0.142	SLUG : 2D-3D TB	633	1803

Table 2. Learjet runs

RUN #	U_{GS} (m/s)	U_{LS} (m/s)	FLOW PATTERNS	Re_L	Re_G
2.1	25.32	0.080	ANNULAR : short roll waves	1016	23224
2.2	0.61	0.084	SLUG : long TB	1067	560
3.1	11.44	0.451	ANNULAR : roll waves	5728	10493
4.1	7.97	0.082	ANNULAR : roll waves	1041	7310
4.2	0.22	0.076	SLUG : 4D TB	965	202
5.1	2.22	0.079	ANNULAR : near transition annular-slug	1003	2036
5.2	0.64	0.080	SLUG : long TB	1016	587
7.1	2.99	0.438	ANNULAR : near transition annular-slug	5563	2742
8.1	1.09	0.460	SLUG : 3D TB ,bubbly slugs	5842	1000
9.1	0.09	0.478	BUBBLE	6071	83
10.1	23.00	0.418	ANNULAR : roll waves	5309	21096
11.1	1.80	0.079	TRANSITION : annular-slug	1003	1651
11.2	1.75	0.45	SLUG : long TB ,bubbly slugs	5715	1605
12.12	1.9	0.92	SLUG : 6D TB,bubbly slugs	11684	1743
13.1	0.7	0.08	SLUG : long TB ,non bubbly slugs	1016	642
13.2	0.65	0.45	SLUG : 2D TB ,bubbly slugs	5715	596
14.1	0.65	0.94	BUBBLE	11938	596
15.1	0.16	0.079	SLUG : 2D 3D TB ,non bubbly slugs	1003	147
15.2	0.13	0.88	BUBBLE	11176	119
16.1.	11.4	0.077	ANNULAR : roll waves	978	10456
16.2	0.134	0.46	BUBBLE	5842	123
17.1	10.1	0.08	ANNULAR : roll waves	1016	9264

3B. Flow is from left to right. At a low gas rate (run 15.1) well-established, stable spherically nosed "Taylor" bubbles which are axisymmetric move along the pipe separated by clear liquid slugs. The back of the bubbles generally assume a shape suggested by Coney & Masica (1969). Bubble and slug lengths vary but the variance is relatively small. As the gas rate is increased the bubbles become longer and in some cases carry very thin membranes which bridge the bubble. Both the bubbles and slugs have much greater variance in length and the slugs contain some gas in the form of dispersed smaller bubbles. At still higher gas rates, as in run 11.1, a condition very close to transition between slug and annular flow appears. Long stretches of nearly smooth film are occasionally disrupted by a slow-moving high-amplitude wave that sometimes is seen to bridge the pipe forming a small liquid slug. In many cases these slugs do not persist, breaking up into a locally thick annular film. Away from the point of slug inception the film is remarkably smooth. At a high gas rate (run 17.1) the film is very wavy with occasional large roll waves sweeping by at velocities approaching the gas velocity.

Figures 4A and 4B show conditions which exist at a much higher liquid flow rate approaching 1 m/s. At the lowest gas rates (run 15.2) the gas is seen to be dispersed in the liquid in the form of bubbles from 0.2 to 0.5 mm in characteristic dimension. At higher gas rates (run 14.1) the bubbles become smaller and more closely packed but still dispersed with what appears to be relative uniformity in the axial direction. However, the next run in this series (run 12.12) displays a high flow rate slug flow. A rapidly moving, highly aerated liquid slug is separated from the next slug by a thick, wavy liquid film which itself carries bubbles. The front and back of the slug are clearly defined even though the degree of aeration is high.

A condition of intermediate gas and liquid rates is shown in figure 5. Here the slug is substantially aerated but the bubbles separating the slugs are regular and their films are free of gas bubbles.

The films and sketches show that these visual observations can provide a great deal of information from which to construct and test simple models for the flow. Conditions of transition can be estimated, the velocity of the slugs and bubbles can be calculated and the variation of these velocities with position of the dispersed bubbles determined. Slug and bubble lengths can be measured for slug flow and some estimate of the bubble size evolved for the distributed bubbly pattern determined. Thus, these flow visualization experiments carry with them much information and this type of analysis is underway at this time. It is already possible to indicate one unexpected result from these observations. During slug flow at 1 G the bubbles carried in the liquid slugs always appear to have a "drift" velocity measured relative to the slug itself. That is, in a coordinate system moving with the slugs the dispersed bubbles appear to move backward. This observation is

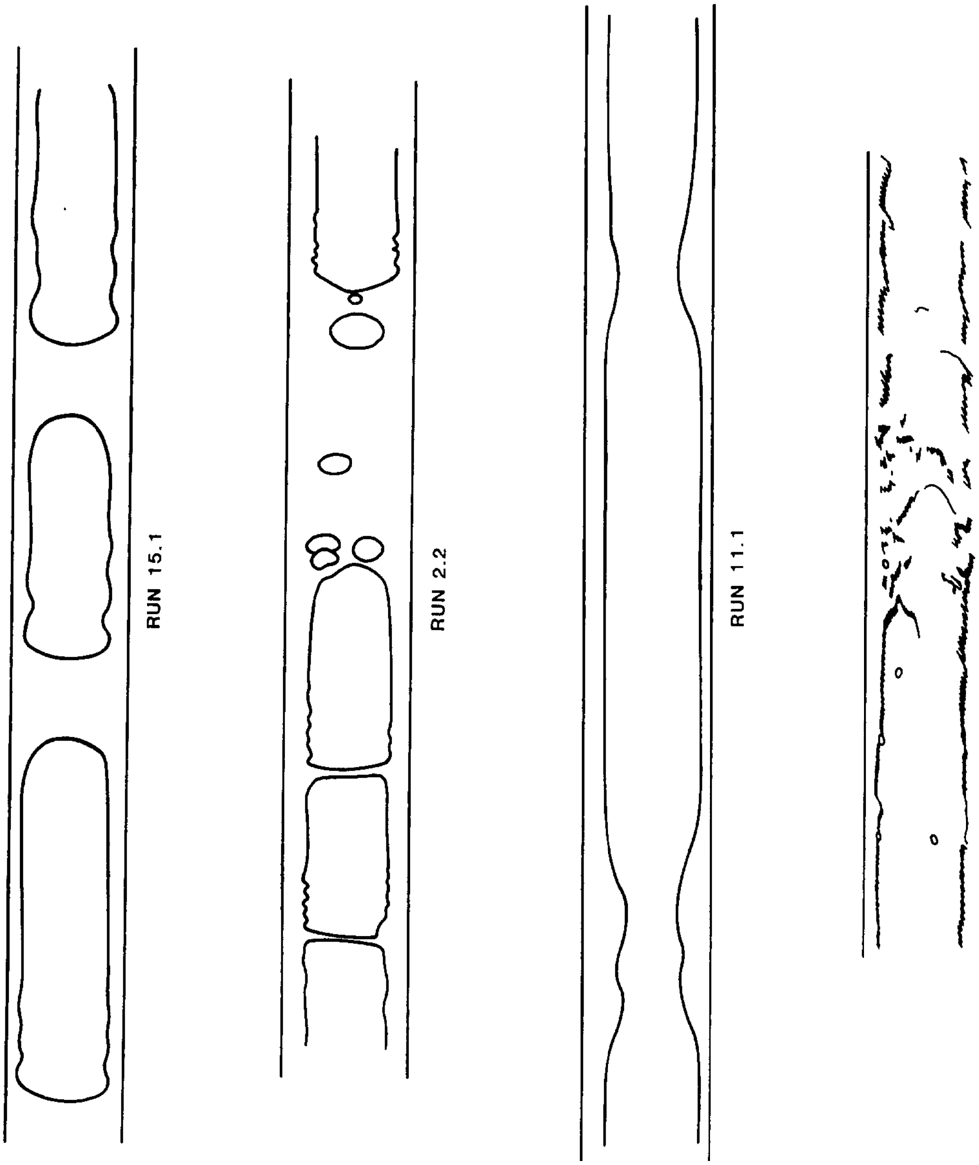

Figure 3B. Sketches of movie frames.

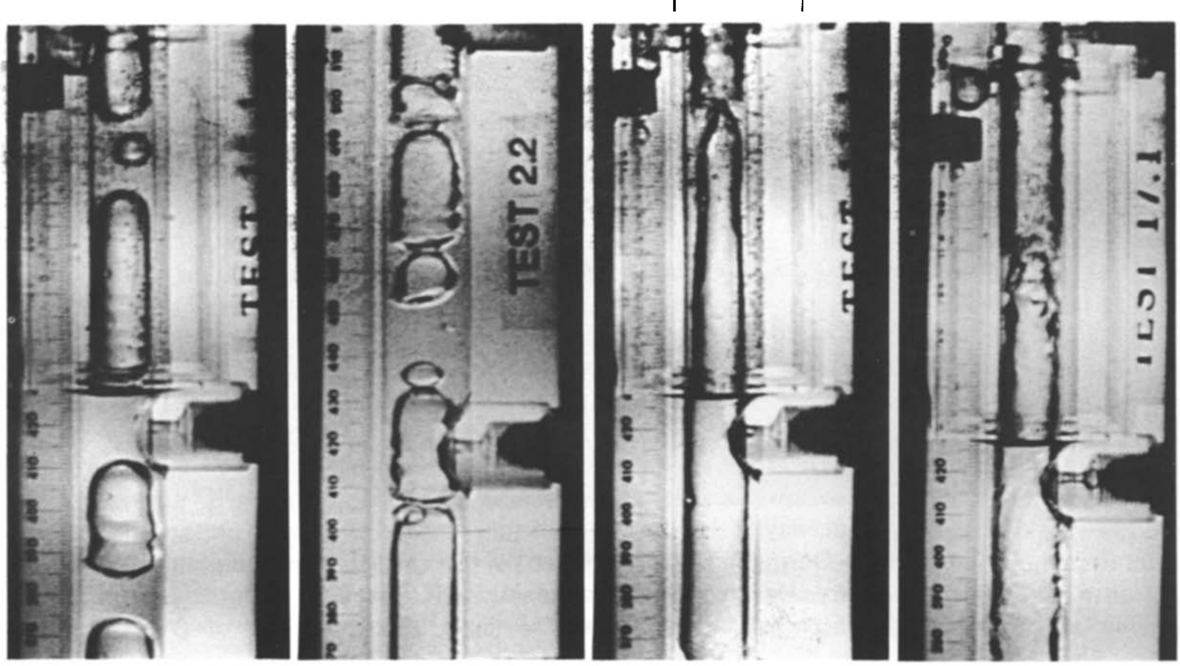

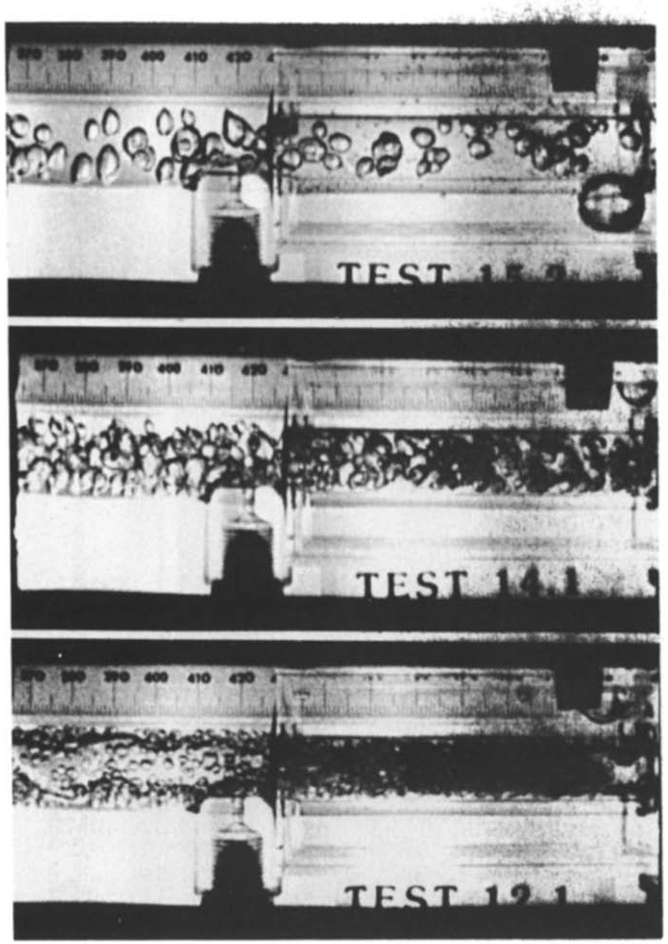

Figure 4A. Single frames from three Learjet runs, $U_{LS} \simeq 0.9$ m/s.

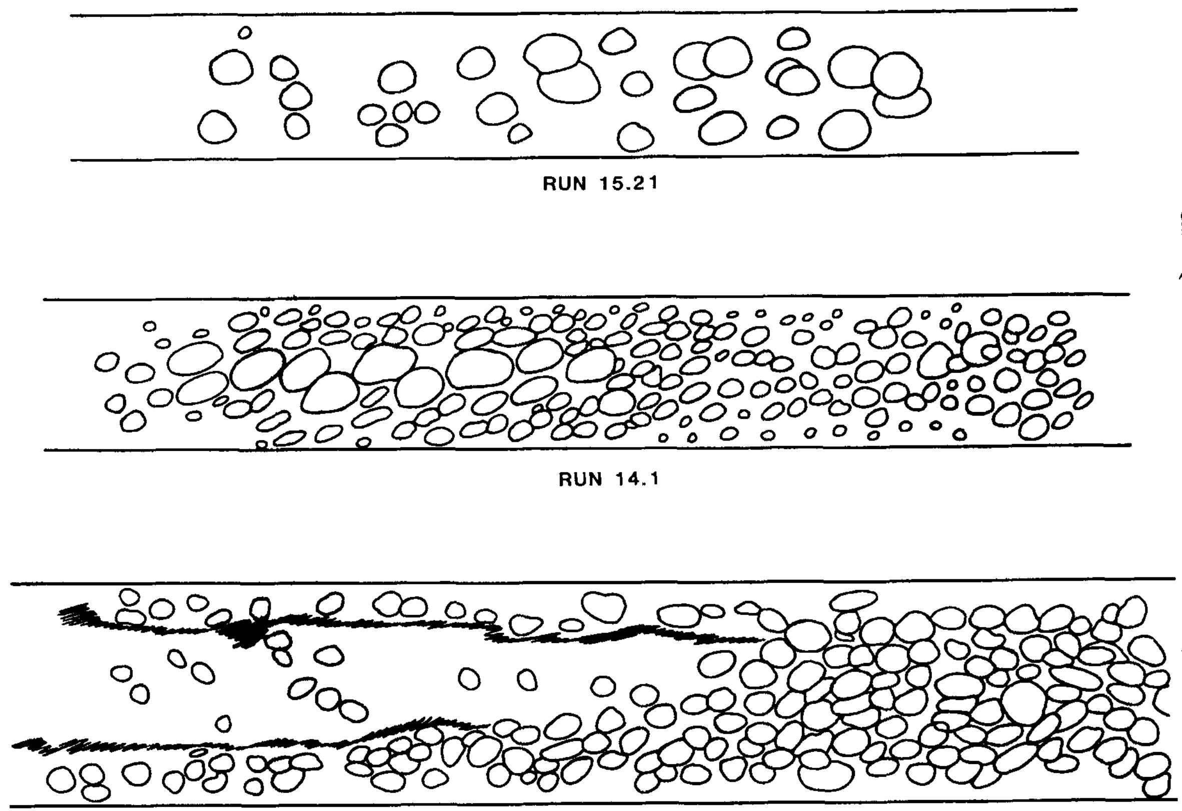

Figure 4B. Sketches of movie frames.

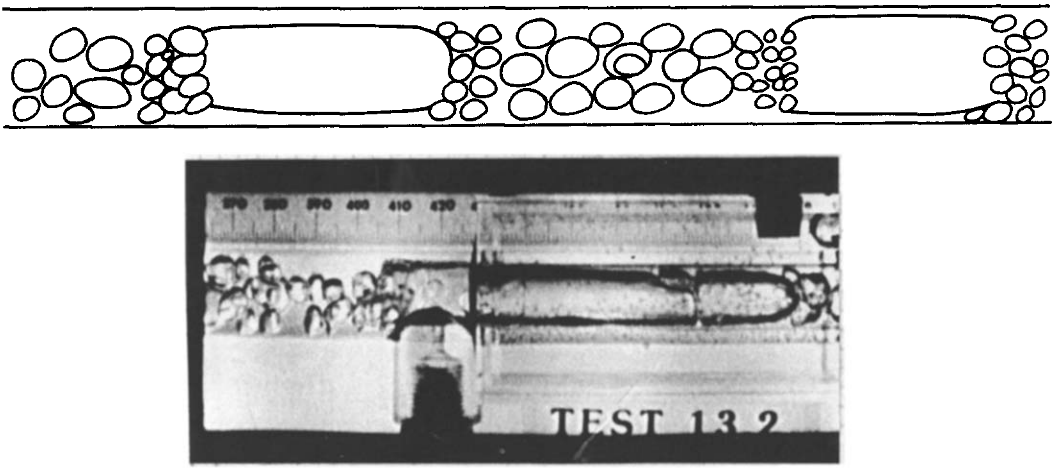

Figure 5. Run 13.2.

consistent with models developed for slug flow in horizontal and vertical pipes (Dukler & Hubbard 1976; Fernandes *et al.* 1983). However, at microgravity conditions these dispersed bubbles move at precisely the velocity of the front of the slug, suggesting that the mechanism of pick up and shedding which has formed the basis of modelling in the past may not be applicable here.

FLOW PATTERN MAPPING

A map of the flow patterns observed is given in figure 6. Data for both the drop tower and the Learjet are included. In general, tube diameter can be expected to have an effect on the location of the transition boundaries in these coordinates of superficial velocity, U_{LS} and U_{GS}. However, in two test section diameters are not drastically different. Furthermore, the drop tower data include only the patterns of bubbly and slug flow and models show that the transition between bubbly and slug flow is relatively insensitive to diameter.

At this time there is debate as to whether the bubble and slug flow regions should be considered as separate patterns or whether this series of runs simply represents a continuum of bubble sizes. At 1 G physical models have been developed which suggest that the mechanism by which the flow takes place changes drastically between these two patterns. However, preliminary analysis for microgravity indicates that these two regions may represent a continuum of the same physical process. If that proves to be the case only two patterns can be considered to characterize the flow, bubbly and annular.

Modelling of the flow pattern transitions is in its earliest stages, however it is possible to suggest some simple ideas by which the location of transition boundaries can be estimated.

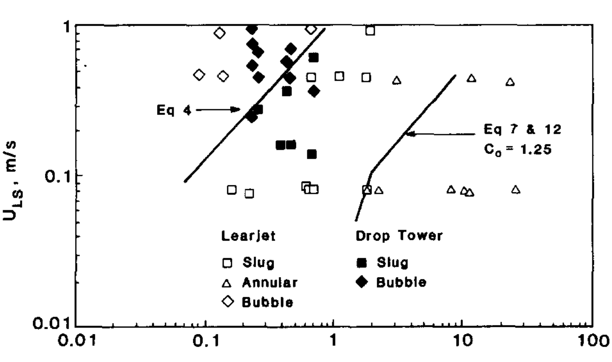

Figure 6. Microgravity flow pattern map. Comparison of data with transition models.

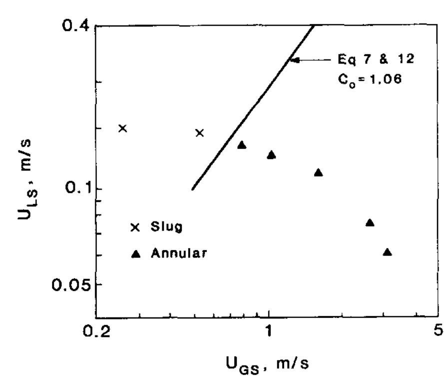

Figure 7. Flow patterns for Sunstrand data. Comparison with transition model.

Bubble to slug pattern

Study of the movie films clearly indicates that the local relative velocity between liquid and gas is negligible. Thus, one can write

$$U_L = U_G, \tag{1}$$

where these are the space-averaged true linear velocities of the liquid and gas, respectively. Designate ϵ as the area average void fraction. The linear velocities and the superficial velocities are related by

$$U_L = \frac{U_{LS}}{1-\epsilon} \text{ and } U_G = \frac{U_{GS}}{\epsilon}, \tag{2}$$

where the superficial velocities are computed as if that phase was flowing alone in the tube. Substituting gives

$$\frac{U_{LS}}{U_{GS}} = \frac{1-\epsilon}{\epsilon}. \tag{3}$$

The transition from bubble to slug flow is thought to take place when the bubble concentration and size is such that adjacent bubbles come into contact. Then coalescence can be expected and surface tension causes the two coalescing bubbles to form one larger one characteristic of slug flow. Thus, one need only estimate the average voids at this condition to obtain an equation relating the superficial velocities at transition. Small bubbles in a cubic array can achieve, at most, a void fraction of 0.52. However, large bubbles, with diameters approaching that of the tube, will generate a holdup before touching which depends on their shape and orientation. For large spherical bubbles this can be shown to be at approx. $\epsilon = 0.5$. However, for ellipsoids the void fraction will depend on whether the major axis is aligned with the axis of the tube or with the radius when the voids will approximate 0.4. Because one observes various alignments, it is speculated that the average void fraction at contact—and thus at transition—is approx. $\epsilon = 0.45$. The resulting equation is then

$$U_{LS} = 1.22\ U_{GS}. \tag{4}$$

This equation is plotted in figure 6 and appears in reasonable agreement with the transition shown by the data. The result is equally satisfactory if $\epsilon = 0.5$ is used. Note that, according to this model, the transition in coordinates of superficial velocity is independent of diameter.

Slug to annular pattern

The following mechanism is hypothesized to take place and cause this transition. During slug flow there is a large axial variation in void fraction between the slugs and the Taylor bubbles. As the gas rate is increased, the length of the bubbles increases relative to the slug lengths. When these slugs become short enough, slight variation in the local velocity or adjacent film thickness can cause the slug to momentarily rupture. Then surface tension forces draw the liquid around the wall of the pipe to establish annular flow and the slug can not be reformed. In order to estimate the flow conditions at which this change will take place equations are developed relating the axial average voids and the superficial flow rates for slug flow. A similar relation is developed for annular flow. It is speculated that the transition between slug and annular flow takes place when the void fraction, as dictated by the former two models, becomes equal. That is, at lower gas velocities, the slug flow model always predicts higher average voids than does the annular flow model at the same flow rates. However, at the transition velocity the voids predicted by the two models are equal. At still higher gas flow rates the slug flow model predicts lower voids than does the annular flow model, and thus the flow pattern becomes one of annular flow since surface tension will cause the liquid to wrap around the wall instead of existing in discrete slugs.

A model for the *average voids in slug flow* can be approached as follows. Consider a typical slug unit consisting of one Taylor bubble of length l_b moving at a velocity U_b and its adjacent slug with corresponding quantities, l_s and U_s. A material balance on the gas gives

$$U_{GS} = U_s \epsilon_s \beta + U_b \epsilon_b (1-\beta), \tag{5}$$

where $\beta = l_s/(l_s + l_b)$. As discussed above, the flow visualization shows that the slug and bubble velocities are equal. Thus, the material balance simplifies to

$$\frac{U_{GS}}{U_b} = \epsilon_s \beta + \alpha_b (1 - \beta) = \langle \epsilon \rangle \qquad [6]$$

and $\langle \epsilon \rangle$ is the average void fraction during slug flow. Modelling of slug flow at microgravity is now underway and should produce a basis for predicting the ratio of the gas superficial velocity to the Taylor bubble velocity. Designate $C_0 = U_b/(U_{LS} + U_{GS})$, which is recognized to be a measure of the rate at which a large bubble advances ahead of the two-phase mixture in slug flow and is a basic parameter in slug flow modelling. Then, substituting into [6], gives

$$\frac{U_{GS}}{U_{LS} + U_{GS}} = C_0 \langle \epsilon \rangle . \qquad [7]$$

Studies of the films show that C_0 ranges between 1.15 and 1.30, depending on the flow rates of the phases. In other systems this ratio may also depend on the fluid properties and pipe size. Until these slug flow modelling studies are completed the average value is assumed to be 1.25, based on analysis of the experiments. Substituting into [6] then provides a relationship between the superficial velocities and average voids in slug flow.

Now consider the condition of *annular flow;* where all of the liquid flows as a smooth film along the wall and the gas flows in the core. A force balance on a control volume bounded by the pipe walls and two planes normal to the axis separated by an axial distance, ΔZ, gives

$$\frac{\Delta P}{\Delta Z} = \frac{4\tau_w}{D}. \qquad [8]$$

The force balance taken over the liquid film in that same control volume is

$$\frac{\Delta P}{\Delta Z}(1 - \epsilon) = \frac{4\tau_w}{D} - \frac{4\tau_i}{D}\epsilon^{1/2}. \qquad [9]$$

In [8] and [9], ΔP is the pressure gradient, τ_w is the wall shear stress and τ_i is the interfacial stress. The pressure gradients in [8] and [9] are equated to give

$$\tau_i = \tau_w \epsilon^{1/2}. \qquad [10]$$

The stresses can be written in friction factor formulation:

$$\tau_i = \frac{f_i \rho_G U_G^2}{2} \text{ and } \tau_w = \frac{f_w \rho_L U_L^2}{2}. \qquad [11]$$

Since $U_L = U_{LS}/(1 - \epsilon)$ and $U_G = U_{GS}/\epsilon$,

$$\frac{\alpha^{5/2}}{(1 - \epsilon)^2} = \left(\frac{f_i}{f_w}\right)\left(\frac{\rho_G}{\rho_L}\right)\left(\frac{U_{GS}}{U_{LS}}\right)^2. \qquad [12]$$

Now it remains only to evaluate each friction factor in terms of the Reynolds number for that phase to arrive at an expression which gives the average voids in annular flow, given the superficial velocities. The Blasius equation for a smooth surface is used for the wall:

$$f_w = \frac{C}{(Re_L)^n}, \qquad [13]$$

where C = 16 when the flow is laminar and 0.046 if turbulent and $n = 1.0$ for laminar flow and 0.2 if turbulent. Little is known at this time about the factors which determine the interfacial friction factor, f_i, except that at the same gas Reynolds number it, is much larger than for flow over a smooth rigid surface. The existence of interfacial waves is known to be the primary cause for this increase, although the precise mechanism of wave action is not yet understood. Experiments on earth show that the details of the wave structure depend on the direction of gravity relative to the direction of flow of the thin film. For purposes of developing this model further at this time, a preliminary estimate of f_i is made using the empirical correlation suggested by Wallis (1969):

$$\frac{f_i}{f_G} = 1 + 150\,(1 - \epsilon^{1/2}), \qquad [14]$$

where f_G is the single-phase friction factor calculated from a relationship similar to [13] with Re_G replacing Re_L.

Now it is possible to evolve the model for transition based on the mechanism suggested above. Equating $\langle \epsilon \rangle$ from [7] with ϵ from [12] provides the intersection between the models for slug flow and annular flow, at which point both models predict the same void fraction. This process, which eliminates α between the two equations, provides a method by which the superficial velocities can be calculated at this transition condition. The result, calculated numerically for the measured value of $C_0 = 1.25$, is shown in figure 6. The discontinuity in the theoretical curve comes as a result of the transition between laminar and turbulent flow. Agreement is seen to be reasonably satisfactory.

A study has recently been completed by Sundstrand on the two-phase flow of Freon-114 at 5.8 b in a transparent pipe, 15.9 mm i.d. during C-135 low-gravity trajectories carried out by the NASA Johnson Space Center. Details of the experiments are available elsewhere (Hill & Downey 1987). These films were provided by NASA and have now been analyzed. Only annular and slug flow patterns were observed. Measurements of the bubble velocities during slug flow showed that $C_0 = 1.06$ for these tests. Theoretical transition boundaries were calculated for this condition and are compared with the Sundstrand data in figure 7, very satisfactory agreement is observed.

It is important to recognize that these results represent preliminary efforts in this transition modelling process. To complete the effort will require a more detailed understanding of slug flow and a basic method of evaluating the effect of interfacial waviness on interfacial shear. This work is in progress and will be reported in due course along with the results of additional experiments currently underway.

Acknowledgements—The support of the National Aeronautics and Space Agency under Grant NAG 3-510 to the University of Houston is gratefully acknowledged.

REFERENCES

ALBERS, J. A. & MACOSKO, R. P. 1965 Experimental pressure drop investigation of non wetting, condensing flow of mercury vapor in a constant diameter tube in 1-G and zero gravity environments. Technical Note NASA TN D-2838.

ALBERS, J. A. & MACOSKO, R. P. 1966 Condensing pressure drop of non wetting mercury in a uniformly tapered tube in 1G and zero gravity environments. Technical Note NASA TN D-3185.

CONEY, T. A. & MASICA, W. J. 1969 Effect of flow rate on the dynamic contact angle for wetting liquids. Technical Note NASA TN D-5115.

DUKLER, A. E. & HUBBARD, M. G. 1976 A model for gas–liquid slug flow in horizontal and near horizontal tubes. *Ind. Engng Chem. Fundam.* **14,** 337–346.

FERNANDES, R., SEMIAT, R. & DUKLER, A. E. 1983 A hydrodynamic model for gas–liquid slug flow in vertical tubes. *AIChE Jl* **29,** 981–989.

HEPNER, D. B., KING, C. D. & LITTLES, J. W. 1975 Zero-G experiments in two-phase fluid flow regimes. ASME Paper 75-ENAs-24.

HEPNER, D. B., KING, C. D. & LITTLES, J. W. 1978 Aircraft flight testing of fluids in zero gravity experiments. General Dynamics Report CASD NAS-74-054.

HILL, D. & DOWNEY, R. S. 1987 A study of two phase flow in a reduced gravity environment. Final Report, Sundstrand Energy Systems under NASA Contract NAS9-17195.

LOVELL, T. K. 1985 Liquid–vapor flow regime transition for use in the design of heat transfer loops in spacecraft: an investigation of two phase flow in zero gravity conditions. AFWAL (Air Force Wright Aeronautical Labs) Report TR-85-3021.

NAMKOONG, D., BLOCK, H. B. & MACOSKO, R. P. 1987 Photographic study of condensing mercury in 0 and 1 G environments. Technical Note NASA TN D-4023.

SIEGAL, R. & USISKIN, C. 1959 A photographic study of boiling in the absence of gravity. *Trans. ASME* **81,** 230–235.

TAITEL, Y. & DUKLER, A. E. 1976 A model for predicting flow regime transitions in horizontal and near horizontal gas–liquid flow. *AIChE Jl* **22,** 47–55.

WALLIS, G. B. 1969 *One Dimensional Two Phase Flows.* McGraw-Hill, New York.

WEINZIERI, A. & STRAUB, J. 1982 Nucleate pool boiling in microgravity environment. *Proc. 7th Int. Heat Transfer Conf.* **4**, 21–27.

WILLIAMS, J. L., KESHOCK, E. G. & WIGGINS, C. L. 1973 Development of a direct condensing radiator for use in a spacecraft vapor compression refrigeration system. *ASME Jl Engng Ind.* **96**, 1053–1063.